

Application of feedforward artificial neural networks to improve process control of PID-based control algorithms

Fernando G. Martins *, Manuel A.N. Coelho

LEP/E, Departamento de Engenharia Química, FEUP, Porto, Portugal

Abstract

The present work reports a new control methodology based on proportional, integral, and derivative (PID) control algorithms conjugated with feedforward artificial neural networks (FANNs). The FANNs were used as predicted models of the controlled variable. This information is transferred to PID controllers, through the readjustment of the pre-established setpoint. The proposed methodology was tested generally for a first order system using a PI controller, a second order system using a PI control, a second order system in series with a first order system using a cascade control structure. The problem of the reaction temperature control in a batch-jacketed reactor with a cascade control structure was also analysed as a particular case. The simulation results shows that better control performances are achieved when the control methodology presented in this work is used as a complementary tool of the PID-based control algorithms. © 2000 Elsevier Science Ltd. All rights reserved.

Keywords: Process control; Feedforward artificial neural networks; Proportional, integral, and derivative based control

1. Introduction

Since the proportional, integral, and derivative (PID) controller finds widespread use in the process industries, great resistances have been occurred to incorporate other control methodologies in practical situations. The main reasons are the simplicity, robustness and successful applications provided by PID-based control structures (Lee, Park, Lee & Brosilow, 1998). However, better performances of the control systems should be achieved to cope new market requirements in product quality, safety procedures and process complexity.

In last few years, artificial neural networks and particularly feedforward artificial neural networks (FANNs) have been extensively studied in academia as process models, and are increasingly being used in industry (Ungar, Hartman, Keeler & Martin, 1996). Artificial neural networks are suggested to generate process models due to their ability to capture nonlinear dynamics. These models are data-driven and have the advantages of computational efficiency and ease of construction (Tsen, Jang & Wong, 1996).

This paper demonstrates one way of how FANNs could be used to accomplish the performance of control structures based on PID controllers. The FANNs are used to create generic models to predict future values of the controlled variable. This information is then incorporated in conventional control system structure through the change of pre-established values of setpoint. The main objective is to enhance the control performance of the control system without change drastically the structure of the control system.

2. Control methodology

The control methodology proposed in this work is based on the conventional control conception (PID-based control structures) conjugated with the development of a model, which is capable of predicting the controlled variable as a function of process measurements and the pre-established setpoint. In this sense, the foreknowledge of the controlled variable value for time $t + \Delta t$ at time t allows to evaluate a second setpoint (pseudo-setpoint) for the principal controller, which can be predicted by the following equation:

$$Sp_t^{\text{new}} = Sp_t^{\text{old}} - k_t(y_{t+\Delta t}^p - Sp_{t+\Delta t}^{\text{old}}) \quad (1)$$

* Corresponding author.

E-mail address: fgm@fe.up.pt (F.G. Martins).

where Sp_t^{new} is the new setpoint at time t , Sp_t^{old} and $Sp_{t+\Delta t}^{old}$ are the pre-established setpoint at time t and at time $t + \Delta t$, respectively, $y_{t+\Delta t}^p$ is the predicted controlled variable, calculated by FANN, k_t is an adjustable parameter and Δt is the time interval between two measurements.

The FANNs models are identified and developed from input–output data. The inputs of the FANNs are the values of the manipulated variable at time t , the values of the load variables at time t , the value of the controlled variable at time t and the pre-established setpoint at time $t + \Delta t$. The output of the FANNs is the predicted value of the controlled variable at time $t + \Delta t$.

The value of k_t is optimised by simulation to cope with setpoint evolution and to avoid simultaneously sudden changes and instabilities in the controlled variable and in final control element.

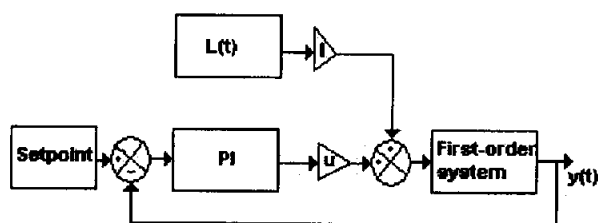


Fig. 1. Block diagram for the first-order system.

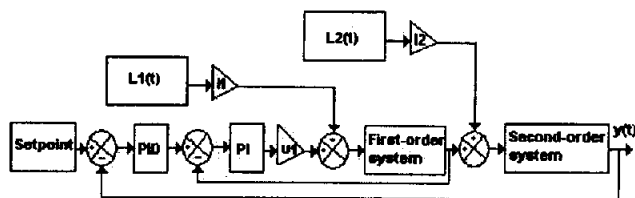


Fig. 2. Block diagram for the first-order system plus a second-order system.

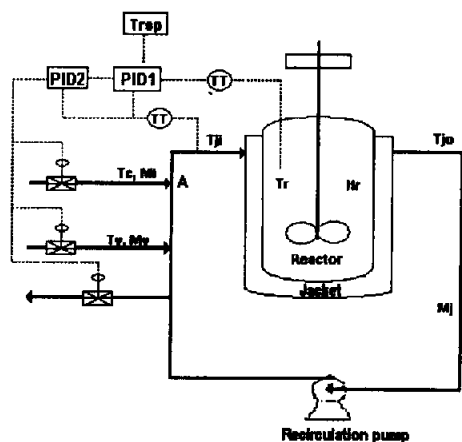


Fig. 3. Schematic representation of the reactor with the heat transfer configuration and cascade control structure.

3. Cases studies

Three examples are considered to analyse, in general terms, the performance of the control methodology proposed in this work. The first is a first-order system with a PI controller, which is represented by the block diagram shown in Fig. 1. The time model for the first-order system is given by:

$$\tau \frac{dy(t)}{dt} + y(t) = lL(t) + uU(t) \quad (2)$$

where $y(t)$ is the controlled variable, τ is the first-order system time constant, $L(t)$ and $U(t)$ are the load and final control element functions, respectively, l and u are constants.

The second case regards a second-order system with a PID controller. The block diagram is similar to the previous one, but with a second-order system and PID controller. For this case, the time model is:

$$\tau^2 \frac{d^2y(t)}{dt^2} + 2\tau\zeta \frac{dy(t)}{dt} + y(t) = lL(t) + uU(t) \quad (3)$$

where ζ is the damping factor and the others variables have the same meaning as defined in the former case.

The third case results from the conjugation of a first order system in series with a second order system using a conventional PID based cascade control structure. The schematic diagram of this process is represented in Fig. 2. $L_1(t)$ and $L_2(t)$ are load functions and l_1 , l_2 and u_1 are constants.

As a practical situation, the proposed control methodology was tested to control the heat transfer process in a batch-jacketed reactor. Fig. 3 shows schematically the reactor with the heat transfer configuration and with the conventional PID-based cascade control structure, commonly used in this type of process.

The model equations were developed attending on the following assumptions,

1. the reactor content is well mixed at all times;
2. jacket heating/cooling occurs, with the heating/cooling medium being well mixed in the jacket;
3. the heat of reaction is known, this variable is generally unknown, but it could be inferred by process measurements;
4. it is assumed that there is not heat loss to the ambient.

The assumptions made above lead to the simplified heat transfer rates:

$$H_t = H_r - m_r C_{p_r} \frac{dT_r}{dt} \quad (4)$$

where H_t is the heat transfer rate to the reactor wall, H_r the heat of reaction rate, m_r the mass of reaction mixture, C_{p_r} the heat capacity of reaction mixture, and T_r is the reaction temperature at time t .

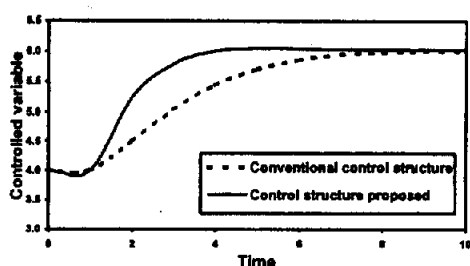


Fig. 4. Closed-loop responses to a 2 units step change in setpoint the first-order system at time equal to 1.

The heat transfer rate to the reactor wall is given by:

$$H_t = h_r A_r (T_r - T_w) \quad (5)$$

where T_w is the reactor wall temperature, h_r the heat transfer coefficient between the reaction mixture and the reactor wall, and A_r is the area of the reactor.

The heat balance to the reactor wall leads to:

$$H_t = \rho_w C_{p_w} V_w \frac{dT}{dt} + h_j A_j (T_w - T_j) \quad (6)$$

where ρ_w , C_{p_w} and V_w are density, heat capacity and volume, of the reactor wall, respectively, h_j the heat transfer coefficient between reactor wall and the jacket fluid, A_j the outside reactor area, and T_j is mean temperature of the fluid in the jacket, given by:

$$T_j = \frac{T_{ji} + T_{jo}}{2} \quad (7)$$

where T_{ji} and T_{jo} are the jacket inlet and jacket outlet fluid temperature, respectively.

Considering that there is not heat accumulation in the jacket, the last term of Eq. (6) can be equalise to:

$$h_j A_j (T_w - T_j) = \rho_j C_{p_j} M_j (T_{jo} - T_{ji}) \quad (8)$$

where ρ_j , C_{p_j} and M_j are, respectively, the density, the heat capacity and the volume flow rate of the jacket fluid.

The heat balance equation to the point A in Fig. 3, leads to:

$$\rho_j C_{p_j} M_j T_{ji} = \rho_j C_{p_j} M_c T_c + \rho_j C_{p_j} (M_j - M_c) T_{jo} \quad (9)$$

where M_c and T_c are the volume flow rate and the temperature of the injected fluid.

4. Results and discussion

All results shown in this section were obtained by simulation. The values of controller's parameters were calculated using the ITAE tuning criterion (Seborg, Edgar & Mellichamp, 1989). The results obtained for all the case studies will be presented with the same logical order. Thus, for each case, it will present the FANNs structure generated, the optimal value of k_r ,

and the comparative results between closed-loop responses of a conventional control structure and the new control methodology proposed.

The simulations concerning the conventional control structures and new approach were performed with the same values of controller's parameters. Therefore, the conventional control structure can be seen as a particular case ($k_r = 0$) of the new control methodology. The values of k_r were also calculated with the ITAE criterion.

The training of FANNs were performed with the non-linear simplex algorithm of Nelder and Mead (Press, Flannery, Teukolsky & Vetterling, 1989). The objective function was to minimize the sum of square errors between the target data and the correspondent values predicted by FANNs during the training phase. The training values were obtained from process model simulation.

4.1. First-order system

The simulations were carried out using the process model given by Eq. (2) with $\tau = 1$, $l = 1$, and $u = 1$. After tuning the PI controller, a database was created with the simulation results obtained from step changes in the setpoint and in the load variables. Several FANNs were trained to achieve a suitable FANN topology, which is able to predict accurate values of the controlled variable.

The artificial neural network consists of an input layer with four nodes, a hidden layer (four nodes) with sigmoid activation functions and an output layer (one node) with linear activation function.

The simulation model of the first-order system coupled with the FANN model incorporated in the control structure allows the calculation of parameter k_r of Eq. (1) by the ITAE criterion. In this case, an optimum value of $k_r = 4$ was found.

The results of the controlled variable evolution for a step change of 2 in the setpoint using the conventional control structure and the new control methodology are plotted in Fig. 4. As can be seen from the figure, the proposed control structure is superior throughout.

To obtain a fair comparison, the closed-loop responses were also calculated for 2 units step change in load variable, keeping the setpoint constant. Fig. 5 shows a plot of these results, which are in agreement with those represented in Fig. 4. It is clearly shown that a better performance can be achieved with the new control methodology.

4.2. Second-order system

In this case, the values of the parameters of Eq. (3) were $\tau = 1$, $l = 1$, $u = 1$, and $\zeta = 0.1$.

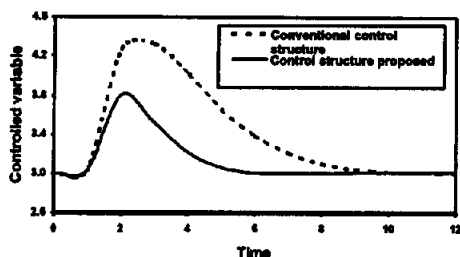


Fig. 5. Closed-loop responses to a 2 units step change in load variable for the first-order system at time equal to 1.

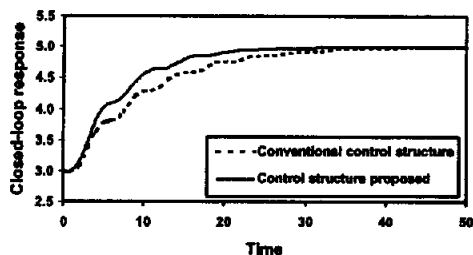


Fig. 6. Closed-loop responses to a 2 units step change in setpoint variable for the second-order system at time equal to 1.

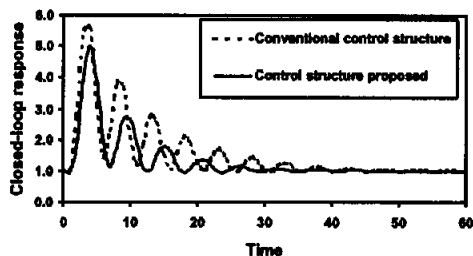


Fig. 7. Closed-loop responses to a 4 units step change in load variable for the second-order system at time equal to 1.

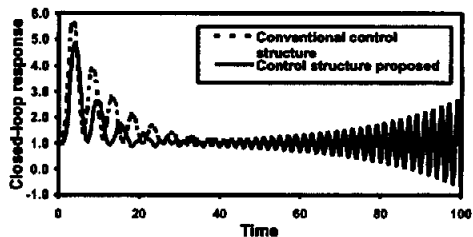


Fig. 8. Closed-loop responses with $k_t = 40$.

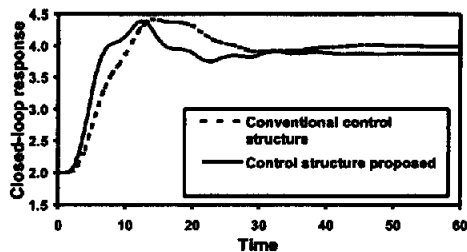


Fig. 9. Closed-loop responses to a 2 units step change in setpoint for a first-order system in series with a second-order system.

The FANN is now composed by three layers with four nodes in input layer, three nodes in hidden layer and one node in output layer. All the activation functions used are linear.

The value of k_t , calculated by the ITAE criterion was 31. The controlled variable evolutions after a step change in the setpoint and load variables are depicted in Figs. 6 and 7, respectively. Analysing these figures, it is observed that the new control method provides better responses than the conventional control structure.

The results of the closed-loop response when the k_t value is greater than the values calculated by ITAE criterion are plotted in Fig. 8. The oscillation behaviour of the closed-loop response observed when the parameter k_t takes higher values than those calculated by ITAE, demonstrate that this criterion is a useful method to estimate the values of the parameter k_t .

4.3. First-order system in series with a second-order system

The simulations were carried out with $l_1 = 1$, $l_2 = 1$, $u_1 = 1$, and $\zeta = 0.1$. The FANN created have three layers with five nodes in the input layer, four sigmoid nodes in the hidden layer and one linear node in the output layer.

The value of k_t , given by the ITAE criterion was 2.9. Fig. 9 depicts the closed-loop response in terms of the main controlled variable evolution when a sudden change in setpoint from 2 to 4 is imposed at time equal to 1. These results demonstrate the improvements achieved with the new approach when compared with the conventional control structure. However, an offset of 0.1 appears with the proposed control structure. This result can be explained by the fact that the FANN generated do not represent well the process in the entire training domain.

The same conclusions are inferred from the Figs. 10 and 11. These figures show the closed-loop responses to a 2 units step changes in loads $L_1(t)$ and $L_2(t)$ (see Fig. 2) at time t equal to 1.

4.4. The heat transfer process on a batch-jacketed reactor

In this case, the FANN consists of three layers with four nodes in the input layer, five sigmoid nodes in the hidden layer and one linear node in the output layer. In the training phase, the four input nodes correspond to the values of heat of reaction (H_r) and the reaction temperature (T_r) at time t , the value of reaction temperature at time $t + \Delta t$ and the value of refrigerated fluid flow rate (M_r) at time $t - \Delta t$. The output node represents the reaction temperature at time $t + \Delta t$.

In the validation phase, the input node representing the reaction temperature at time $t + \Delta t$ was replaced by

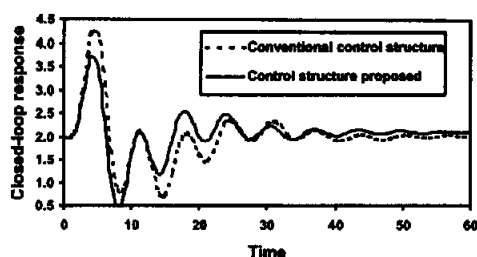


Fig. 10. Closed-loop responses to a 2 units step change in input load $L_1(t)$ for a first-order in series with a second-order system.

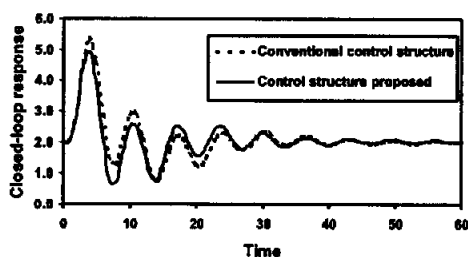


Fig. 11. Closed-loop responses to a 2 units in input load $L_2(t)$ for a first-order system in series with a second-order system.

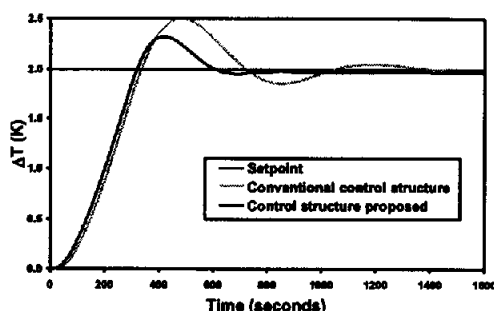


Fig. 12. Reaction temperature evolution after a step change of 2 K in reaction temperature setpoint.

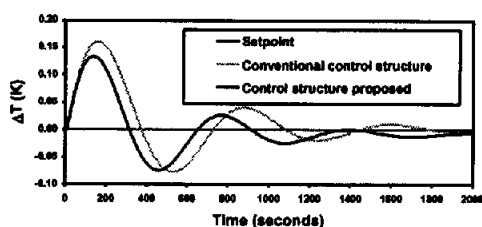


Fig. 13. Deviation of reaction temperature from setpoint after a step change of 20% in the heat of reaction.

the pre-established setpoint value at time $t + \Delta t$. The value of k_t for this system was 3.2. Fig. 12 shows the reaction temperature evolution after a step change of 2 K in the reaction temperature setpoint. It was observed that the time needed to reach the new setpoint is significantly reduced with the new control methodology if compared with the 1200 s required with the conventional control structure.

Fig. 13 shows the deviation of reaction temperature from the setpoint after a step change of 20% in the heat of reaction. The superior performance of the proposed method is readily apparent from this figure.

5. Conclusions

This work shows how it is possible to improve the performance of PID-based control systems without drastically changes the conventional control structure. The efficiency of feedforward artificial neural networks actuating as process models to predict future values of controlled variables was also demonstrated from results. The advantage is that FANNs integrate process data and associated noise. The input/output data is obtained from the system and these values are used in the training phase. However FANNs are trained models and not programmed models. The values of the input and output data available for training must characterise very well the system. The application of FANNs outside training boundary values should be careful analysed.

For all case studies, developed in this work, the performance of the control methodology proposed was superior throughout in terms of tracking setpoint and settling time. However, it is pertinent to say that this control methodology must be tested on pilot and/or industrial scale to obtain experimental validation of the control methodology discussed.

6. Nomenclature

A_r	jacket effective heat transfer area (m^2)
C_p	heat capacity of reaction mixture (J/kg K)
C_{p_j}	specific heat of the jacket and injected fluid (water) (J/kg K)
C_{p_w}	heat capacity of reactor material (J/kg K)
h_i	heat transfer coefficient between the reactor wall and the fluid in the reactor ($\text{W/m}^2 \text{K}$)
h_j	heat transfer coefficient between the jacket fluid and the reactor wall ($\text{W/m}^2 \text{K}$)
H_j	heat transfer rate in the jacket (W)
H_r	heat of reaction rate (W)
H_t	rate of the heat absorbed by the jacket fluid (W)
$L(t)$	load variable
$L_1(t)$	load variable
$L_2(t)$	load variable
m	mass of the mixture in the reactor (kg)
m_w	mass of reactor material (kg)

M_i	injected refrigerated fluid flow rate (m^3/s)
M_j	jacket fluid flow rate (m^3/s)
M_v	injected hot fluid flow rate in jacket (m^3/s)
Sp_t^{new}	new setpoint at time t
Sp_t^{old}	pre-established setpoint at time t
$Sp_{t+\Delta t}^{\text{old}}$	pre-established setpoint at time $t + \Delta t$
t	time (s)
T_j	mean temperature of the jacket fluid (K)
T_{ji}	inlet jacket fluid temperature (K)
T_{jo}	outlet jacket fluid temperature (K)
T_r	reaction temperature (K)
T_w	reactor wall temperature (K)
U	overall heat transfer coefficient (jacket) ($\text{W}/\text{m}^2 \text{K}$)
u, l, l_1, l_2	constants
$u(t)$	final control element
V_w	volume of the reactor wall
$y(t)$	controlled variable
$y_{t+\Delta t}^p$	predicted controlled variable
<i>Greek letters</i>	
Δt	time interval
ρ_j	density of the water and the refrigerated fluid (kg/m^3)
ρ_w	density of the reactor wall kg/m^3

τ	time constants
ζ	damping factor

Acknowledgements

This work was partially supported by JNICT and Praxis XXI under grant RM-2515/93 and Agência de Inovação under project Galporto21.

References

- Lee, Y., Park, S., Lee, M., & Brosilow, C. (1998). PID controller tuning for desired closed-loop responses for SISO systems. *American Institute of Chemical Engineering Journal*, 44(1), 106–115.
- Press, W. H., Flannery, B. P., Teukolsky, S. A., & Vetterling, W. T. (1989). *Numerical recipes — the art of scientific computing (Fortran version)*. Cambridge: Cambridge University Press.
- Seborg, D. E., Edgar, T. F., & Mellichamp, D. A. (1989). *Process dynamics and control*. New York: Wiley.
- Tsen, A. Y.-D., Jang, S. S., & Wong, D. S. H. (1996). Predictive control of quality in batch polymerization using hybrid ANN models. *American Institute of Chemical Engineering Journal*, 42(2), 455–465.
- Ungar, L. H., Hartman, E. J., Keeler, J. D., & Martin, G. D. (1996). Process modelling and control using neural networks. *American Institute of Chemical Engineers Symposium Series*, 92, 57–66.